BILINGUAL PUBLISHING CO.
Pioneer of Global Academics Since 1984

Organic Polymer Material Research
https://ojs.bilpublishing.com/index.php/opmr

ARTICLE

ATR-FTIR Analysis on Aliphatic Hydrocarbon Bond (C-H) Formation and Carboxyl Content during the Ageing of DC Air Plasma Treated Cotton Cellulose and Its Impact on Hydrophilicity

S. Anitha[1*] K. Vaideki[2]

1. Department of Basic Science (Physics), PSG Polytechnic College, Coimbatore, India
2. Department of Applied Science, PSG College of Technology, Coimbatore, India

ARTICLE INFO

Article history
Received: 8 April 2022
Revised: 18 May 2022
Accepted: 7 June 2022
Published Online: 14 June 2022

Keywords:
Cotton cellulose
DC air plasma process
Ageing of sample
Aliphatic hydrocarbon bond (C-H) formation
Carboxyl content

ABSTRACT

The surface of the cotton fabric was modified using a direct current (DC) air plasma treatment and hence enhances its hydrophilicity. The Box-Behnken approach (design expert software) was used to optimise the input process parameters. The sample prepared under optimized condition is subjected to ATR-FTIR and Field Emission Scanning Electron Microscopy (FESEM) studies in order to determine the changes in hydrogen bond energies (EH), Total Crystallinity Index (TCI), Hydrogen Bond Intensity (HBI), Lateral Order Index (LOI), functionalization, lattice parameters (a, b, c & β), degree of crystallinity (in %) and surface etching. The ageing of this sample has been studied by comparing the values of carboxyl content and AC-C/AC-O-C ratio calculated using data extracted from ATR-FTIR spectra of the sample recorded periodically for one month.

1. Introduction

Many researchers have reported the structure and the properties of the cotton fabric have been modified by plasma treatment. Plasma treatment of the cellulosic material modifies the surface thus changes the physical and chemical property of the fabric. Chemical and physical changes induce crystallinity changes, oxidation and etching of the sample. These physical and chemical modifications will enhance the wickability of cellulose materials after plasma treatment. In addition, when the fabric is subjected to plasma treatment carboxyl groups content present in the fabric increases thereby creates the channel for water penetration [1].

Fourier transform infrared spectroscopy and X-ray diffractogram are being increasingly used to carry out both qualitative and quantitative characterization of cellulose and cellulosic materials. Several articles on infrared spec-

**Corresponding Author:*
S. Anitha,
Department of Basic Science (Physics), PSG Polytechnic College, Coimbatore, India;
Email: vp.anitha@gmail.com

DOI: https://doi.org/10.30564/opmr.v4i1.4610

troscopy examination of native cotton have been published. FTIR spectroscopy is essential to obtain information about the hydrogen bonds and establish a relationship between the spectrum of hydroxyl groups and the crystallinity of cellulose [2].

Khai *et al.* (2017) [3] have explained the use of FTIR to evaluate the structural characteristic from the intensity of the characteristic bands. By comparing the peak of a functional group within crystalline domain with the peak of some other functional group in the amorphous domain in the FTIR analysis, the amount of crystalline and amorphous nature in cellulose can be determined. The shift and shape of the characteristic bands are used to research the transformation of cellulose structure.

O'Connor *et al.* (1958) [4] established the empirical "Crystallinity Index" for native cotton, wherein the authors explained the variation in a ratio-based crystallinity index absorption at 1429 cm^{-1} (CH_2 scissoring at C(6) in cellulose) and 893 cm^{-1} (C–O–C valence vibration of β-glycosidic link). Later, the authors (Nelson and O'Connor 1964b) [5], developed the absorption ratio at 1372 cm^{-1} (C–H deformation in cellulose) to 2900 cm^{-1} (C-H stretching) as the "Total Crystalline Index" to study the degree of crystallinity of cellulose.

Gaur *et al.* (2017) [6] related the degree of intermolecular regularity with the Hydrogen Bond Intensity (HBI). HBI of the cellulose sample are the proportion between the absorbance bands at 3400 cm^{-1} (H-bonded absorption) to 1320 cm^{-1} (CH_2 rocking vibration). The authors explained that the reason for reduction in HBI is due to the weakening or reorganization of H-bonds between glucan chains or inside the chain due to thermal treatments.

Poletto *et al.* (2014) [7] used FTIR spectroscopy in order to quickly learn about the structure of cellulose. The structural and chemical shifts in cellulose that occur as a result of different treatments have been correlated with Hydrogen Bond Intensity (HBI), Lateral Order Index (LOI) and Total Crystallinity Index (TCI) values.

M. El-Zawahry and N. A. Ibrahim (2006) [8] have carried out studies on the effect of ageing on Nitrogen plasma-treated wool fabric. It was noted that there is a a small reduction in the amount of acid dye uptake storage period of 100 hours which was ascribed resulting in the creation of additional anionic sites on the surface of the treated wool and as a result of anionic repulsion at the wool fibre surface, the electro negativity of the wool surface increases, and the tendency to absorb dye anions decreases. Another reason proposed by the authors was that because of the mobility of macromolecular segments, plasma-formed functional groups from the surface layer may be removed from the wool structure, reducing its ability to pick up dye anion.

N. Reza M.A. Malek and Ian Holme (2003) [9] studied the ageing process of cotton fiber after oxygen plasma treatment. The results show that during ageing process the oxidation of samples promoted more carboxyl groups on the fibres which would lead to higher electronegative surface potential. This leads to electrostatic repulsion of the direct dye anions and a decrease in the uptake of such a dye by the oxidized fibers.

In this line, this paper studies the impact of DC air plasma treatment on the surface oxidation and the hydrophilicity of cotton cellulose. ATR-FTIR spectroscopy is used to study the structural changes in cotton cellulose after the air plasma treatment. To evaluate the ageing process of treated cotton cellulose, the stability of free radicals formed on the surface of cotton cellulose as a result of air plasma modification was studied.

ATR-FTIR spectroscopy is employed to study the structural changes due to the plasma treatment and hence the increase in hydrophilicity due to structural changes. The evaluation of ageing process of DC air plasma modified cotton cellulose has been carried to study the stability of free radicals created on the cotton cellulose.

2. Experimental Methods

2.1 Cotton Fabric

Plain weave fabric made of 100 percent pure cotton with a warp count of Ne 22 and Ne 19's weft count was used in the current study. The EPI and PPI of the fabric are found to be 68 × 55, with the thickness of 0.36 mm and surface mass of 160 GSM. To remove starch, the cotton cloth was first soaked in boiling water for an hour and then air dried. Afterwards, the fabric was pressed on an industrial scale (Ironing).

2.2 DC Air Plasma Treatment

The electrodes and DC plasma chamber were made up of Stainless steel. The chamber was attached to the rotary pump, and the fabric sample of 20 cm × 20 cm was hooked between electrodes (Hind Hivac). In the presence of the fabric, the lowest possible base pressure was 0.2 millibar. The plasma chamber was shown in a schematic diagram in Figure 1.

Electrode gap, process gas pressure, DC current, and plasma exposure period were the process parameters that could be changed during plasma treatment. As a result, the parameters must be tweaked in order to achieve high hydrophilicity.

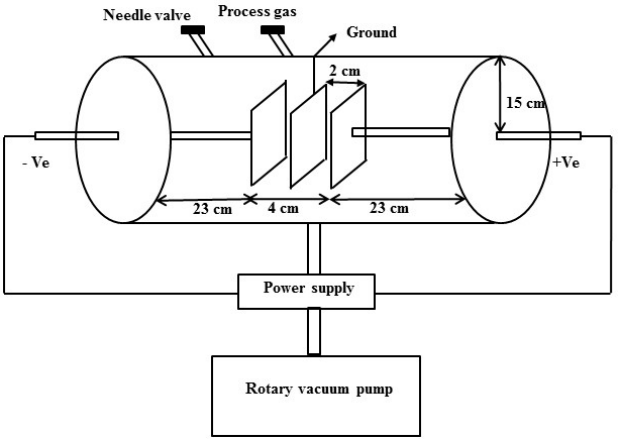

Figure 1. Schematic diagram of DC plasma chamber

2.3 Assessment of Hydrophilicity

The hydrophilicity of the untreated and DC air plasma treated samples was determined by employing the dynamic wicking test (BS 4554) to determine the wicking height (method of test for wettability of textile fabrics 1970). The average wicking height was determined by laying a strip of (2 cm × 20 cm) fabric vertically with its edge in contact with the distilled water and taking readings for five strips of the same sample. The rise in water level (wicking height) observed after 45 minutes was used to determine hydrophilicity.

The mean pore radius was determined using a modified Lucas Washburn equation and a dynamic wicking test (1) [10,11]. A graph is drawn between L^2 vs t, slope of the line gives the mean pore radius.

$$L^2 = \left(\frac{R\gamma}{2\eta}\right)t \tag{1}$$

where,
L – wicking height,
R – mean pore radius,
η – coefficient of viscosity of the liquid,
γ – surface tension of the liquid,
t – time taken for wicking.

2.4 ATR-FTIR Analysis

ATR-FTIR spectra were used to examine the chemical changes on the fabric surface caused by various procedures. A FTIR spectrometer (Perkin Elmer, USA, Spectrum Two) was used to capture the spectrum in the band of 4000 cm^{-1}~500 cm^{-1} with a 4 cm^{-1} resolution and 64 scans. The intensity values of peak heights were used to calculate the three standard crystallinity indices namely Hydrogen Bond Intensity (HBI), Total Crystallinity Index (TCI) and Lateral Order Index (LOI) described in literature [5,11]. IR spectral data was used to calculate the three indices, as well as hydrogen bond energy (E_H) and hydrogen bond distances (B_L).

The energy of hydrogen bonding (EH) was calculated using Struszczyk and Poletto's Equation (2) [7,12] as follows:

$$E_H = \frac{1}{k}\left(\frac{\nu_o - \nu}{\nu_o}\right) \tag{2}$$

where,
νo = standard frequency corresponding to free OH groups (3650 cm^{-1});
ν = frequency of the bonded OH groups;
k is a constant (1/ k = 2.625 × 10^2 kJ).

The hydrogen bond distances (B_L) for OH stretching bands was calculated using Equation (3) [7,13].

$$\Delta\nu\ (cm^{-1}) = 4430 \times (2.84 - B_L)$$
$$\Delta\nu = \nu_o - \nu \tag{3}$$

where,
ν_0 = monomeric OH stretching frequency, (3600 cm^{-1});
ν = stretching frequency observed in the infrared spectrum of the sample.

Lateral Order Index (LOI) proposed by Nelson and O'Connor [5] was used to evaluate the orderliness in cellulose and it was found using Equation (4).

$$\text{LOI} = \frac{A1430}{A898} \tag{4}$$

The IR spectra were used for the calculation of the Hydrogen Bond Intensity (HBI, A3400/A1320) proposed by (Nada *et al.* 2000) [14] and Total Crystallinity Index (TCI, A1372/A2900) proposed by (Nelson & O'Connor 1964) [5].
where,
A1430 - Intensity of A1430 cm^{-1} peak CH_2 scissoring at C_6 in cellulose;
A898 - Intensity of A898 cm^{-1} peak C-O-C valence vibration of β-glycosidic link;
A3400 - Intensity of 3400 cm^{-1} peak (O(2)H···O(6));
A1320 - Intensity of 1320 cm^{-1} peak (CH_2 wagging);
A1372 - Intensity of 1372 cm^{-1} peak (C–H deformation in cellulose);
A2900 - Intensity of 2900 cm^{-1} peak (CH_2 stretching in cellulose from C6).

2.5 FESEM Analysis

Etching and the creation of micro holes are two of the physical changes that the plasma treatment causes on the fabric surface. A Field Emission Scanning Electron Microscope was used to examine the surface morphology of the untreated and plasma-treated samples (Carl Zeiss, UK, SIGMA). The fabric samples were initially treated with

gold to prevent charging effects. Micrographs were taken at a magnification of 50000× for a 3 kV acceleration voltage.

2.6 Estimation of Concentration of Carboxyl Group-Sodium Bicarbonate-Sodium Chloride Test

The TAPPI (Technical Association of Pulp and Paper Industry) standard test for determining carboxyl group concentration in cotton fibres is the sodium bicarbonate-sodium chloride test [15]. The cotton sample is extracted with dilute hydrochloric acid in this process (0.1 M). The material is then filtered after being rinsed with distilled water and reacting with a 0.01 M sodium bicarbonate –0.1M sodium chloride solution. The filtrate is then titrated with 0.01 M hydrochloric acid while methyl red is used as an indicator. The formula is used to compute the carboxyl group concentration in meq/100 g.

Concentration of carboxyl group (meq/100 g)=

$$\left[B-\left(A+\frac{A\times C}{50}\right)\times M\times\frac{200}{W}\right] \quad (5)$$

where,

C - weight of water in wet fabric in grams;

W - oven dry weight of the sample in grams;

A - volume of 0.01 M HCl required to titrate 25 mL of the sample solution in mL;

M - Molarity of HCl used for titration;

B - volume of 0.01 M HCl required to titrate 25 mL of the sodium bicarbonate-sodium chloride original solution;

2 - factor for the used volume ratio between sodium bicarbonate-sodium chloride solution and filtrate used in the test;

50 - volume of sodium bicarbonate-sodium chloride solution used in the test.

3. Results and Discussions

The Box-Behnken design of experiment was used to optimise the parameters of the DC air plasma process. The optimization is carried out to attain the highest possible hydrophilicity in DC plasma treated samples for the parameters that have already been described in our earlier research [16]. The optimal process parameters for DC air plasma treatment are obtained when the gas pressure is 0.5 mbar, the treatment time is 15 minutes, and the DC current is 25 mA. The wicking response observed experimentally is 12.60 cm, compared to 9.4 cm for untreated fabric, indicating a (25 percent) increase in hydrophilicity.

The optimised sample is subjected to ATR-FTIR and FESEM analysis to study the structural and morphological changes of cellulose fabric surface due to DC air plasma treatment. Ageing analysis has been carried out for the optimised sample to ascertain the factors affecting the samples under stored conditions.

3.1 ATR-FTIR Analysis of Optimised Sample

To explore the effect of plasma surface modification in promoting capillarity action, the ATR-FTIR spectra of untreated (control) and plasma treated fabric (Figure 2) were compared. The spectral alterations after plasma therapy were compared to those described in the literature, and the results are shown in Table 1.

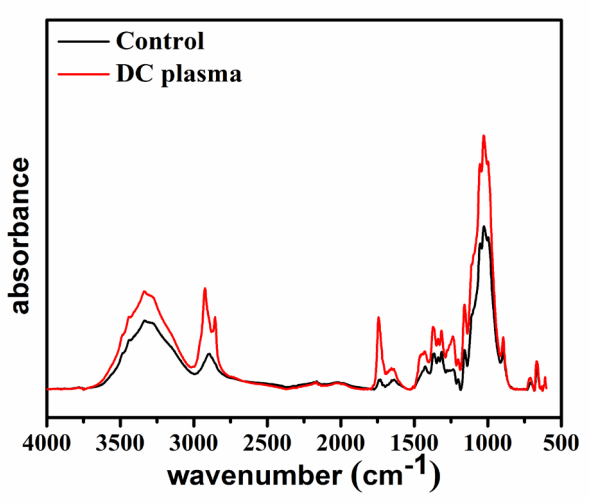

Figure 2. ATR-FTIR spectra of control and DC air plasma (optimised process parameters) treated sample

As discussed in earlier sections, the hydroxyl stretching region is crucial for understanding the hydrogen bonding systems. The OH stretching band covers 3-4 sub peaks i.e. the intermolecular hydrogen bond O6H···O3, intramolecular hydrogen bond O3H···O5 and O2H···O6 respectively. However, the bands corresponding to inter, intra and intersheet hydrogen bonds can only be noticed in the second derivative in most cases of the FTIR spectrum which the original data set does not allow for and hence deconvolution is used to determine the exact location of the peak of hydrogen bonds. This method of deconvolution enhances the resolution and even small difference in the spectrum can be identified. Similarly four sub peaks between 3000 cm^{-1} ~ 2800 cm^{-1} and 1740 cm^{-1} ~ 1710 cm^{-1} are identified by deconvolution method. The peak positions are discussed in the Table 1 and presented in the Figure 3 respectively.

The spectral changes in the above said peaks are discussed and related with the structural changes after plasma treatment.

Table 1. IR frequency of control and DC air plasma treated sample

Wavenumber (cm^{-1}) literature	Wavenumber (cm^{-1}) control fabric	Wavenumber (cm^{-1}) DC plasma treated fabric	Interpretation
3455–3410 (3420)	3456	3454	O2H···O6 intramolecular hydrogen bond in cellulose
3375–3340	3335	3339	O3H···O5 intramolecular hydrogen bond in cellulose
3310–3230	3255	3273	O6H···O3 intermolecular hydrogen bond in cellulose
2981–2933	2952	-	Asymmetric CH_2 valence vibration
2940–2850	2898 2870	2901 2874	Symmetric CH_2 valence vibration
2980–2835	2918 2853	2925 2856	Ring CH, CH_2,CH_2OH in cellulose from C6
1738–1709	1741 1728 1720 1710	1742 1730 1720 1712	C=O stretch in unconjugated ketones, carbonyls, esters.
1685–1655	1655	1655	C=O stretch
1636	1638	1638	Adsorbed water
1594 and 1558	-	1599	C=O stretch
1435	-	1431	H–O–C bending
1430–1416 (1420)	1425	1431	CH_2 scissoring at C(6) in cellulose
1376–1372 (1374)	1370	1370	C–H deformation in cellulose
1364	1364	1364	Symmetric C–H bending
1338–1335	1336	1338	O–H in-plain deformation
1316	1315	1316	CH_2 wagging
1282–1277	1261	1261	C–H deformation
1235–1225	1236	1237	O–H in-plain deformation at C(6)
1205–1200	1201	1202	O–H in-plain deformation
1162–1125 (1159)	1159	1159	C–O–C asymmetric from β-glycosidic link in cellulose
1110	1110	1110	Ring asymmetric valence vibration
1060–1015 (1170)	1053	1053	C–O vibration mainly from C(3)···O(3)H in cellulose II
1035–1030	1027	1027	C–O stretching
996–985	997	997	C–O valence vibration at C(6)
896–892 (899)	895	895	C–O–C valence vibration of β-glycosidic link
670–668	665	665	O–H out-of-plane bending

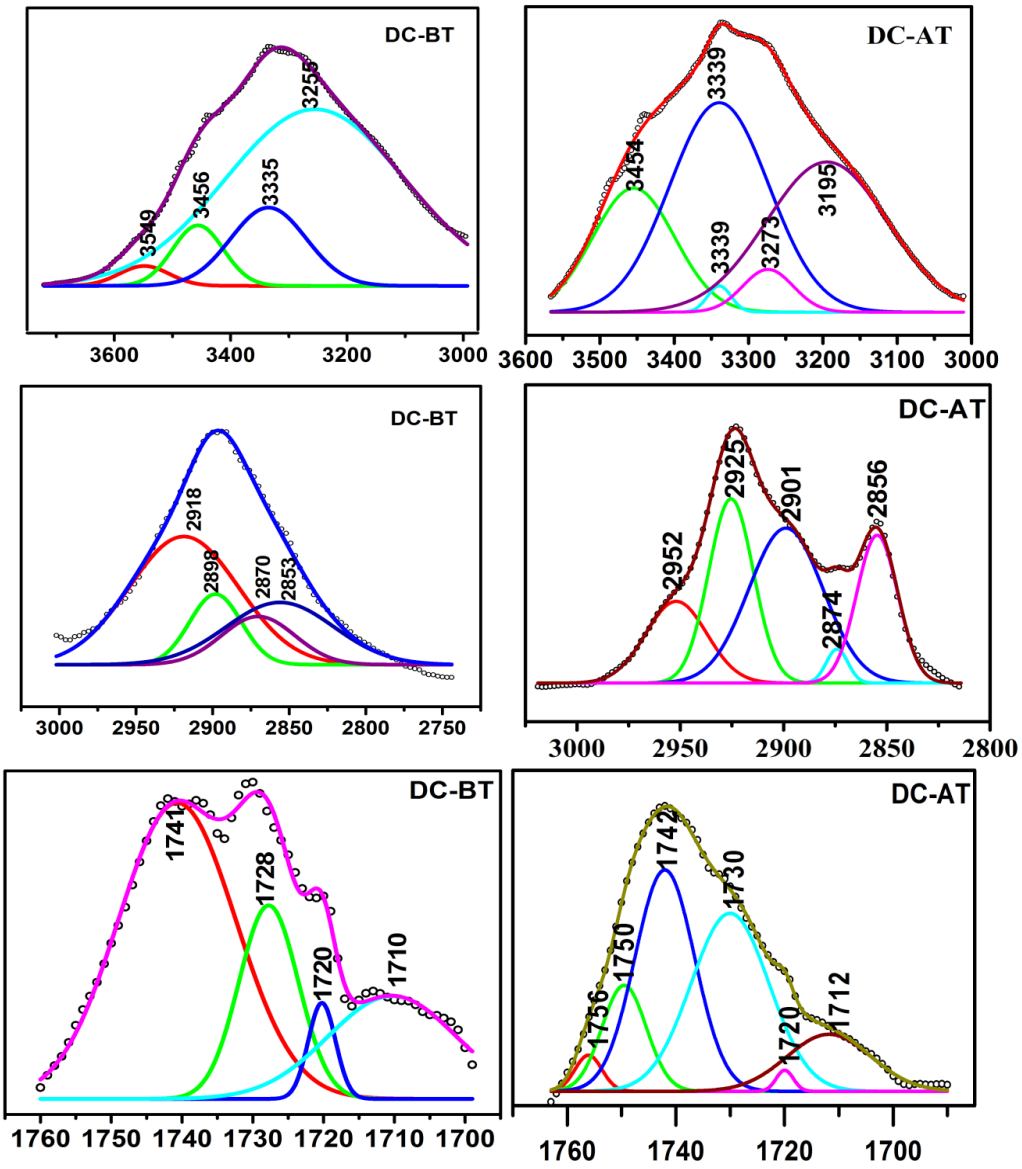

Figure 3. Deconvoluted spectra of control and DC air plasma (optimised process parameters) treated sample

The bond energies of hydrogen bond, LOI, TCI, HBI were calculated for the pre-treated and post treated samples and the results are presented in Table 2. Hence the increase in wicking ability has been discussed based on the results obtained.

In the unit cell of cellulose, the intermolecular hydrogen bond O6H···O3 lies along the

"b" axis, intramolecular hydrogen bonding O3H···O5, O2H···O6 which is parallel to glycosidic linkage C-O-C lies along "c" axis and the intersheet hydrogen bonding lies along "a" axis. Overall strains in the cellulose have been correlated with the wave number shift of intra and inter molecular hydrogen bonding. The shift in frequency of hydrogen bond changes the bond energy of the hydrogen bond and these changes induce strain in the cellulose promoting hydrophilicity.

It can be inferred from the Table 2, that the bond energies of all the hydrogen bond increases except for intramolecular hydrogen bond O2H···O6 decreases after DC air plasma treatment. The peak at 3255 cm^{-1} corresponding to O(6)H stretching (str) is shifted to 3273 cm^{-1} after plasma treatment that indicated an increase in bond energy of OH stretching and hence a decrease in bond length which resulted in the weakening of the O6H···O3 intermolecular hydrogen bond. Similarly the peak corresponding to C_6H_2 symmetric CH_2 valence vibration was shifted from 2898 cm^{-1} to 2901 cm^{-1} representing the shortening of the C-H bond which would result in the rotation of C5-C6 bond. The

Table 2. Hydrogen bond energy, LOI, TCI, HBI and intensity of acid groups of DC air plasma (optimised process parameters) treated sample

Bond energy and Bond length												
Process Parameters			**Intermolecular O6H···O3**		**Intramolecular O3H···O5**		**Intramolecular O2H···O6**		**Intersheet hydrogen bond (C – H···O)**		**Intersheet hydrogen bond (C – H···O)**	
P	**I**	**t**	**(3230-3310)**		**(3340-3375)**		**(3405-3460)**		**2920**		**2850**	
			ΔB_L (Å)	ΔE_H (kJ)	ΔB_L (Å)	ΔE_H (kJ)	ΔB_L (Å)	ΔE_H (kJ)	ΔB_L (Å)	ΔE_H (kJ)	ΔB_L (Å)	ΔE_H (kJ)
0.5	25	15	–0.0041	1.2945	–0.2877	0.0719	0.0005	–0.1438	–0.0016	0.5034	–0.0007	0.2158

TCI, LOI and HBI												
Process Parameters			**IR Crystallinity Ratio**			**Lateral order index**			**Hydrogen bond intensity**			**WH**
P	**I**	**t**	**TCI (A1372/A2900)**			**LOI (A1429/A893)**			**HBI (A3400/A1320)**			
0.5	25	15	0.71	0.47	0.24	0.57	0.41	0.16	3.23	1.67	1.56	12.60

Process parameters			**Physical and Chemical analysis**								
P	**I**	**t**	**WH (cm)**	**Intensity of C=O stretching**							
				Aldehyde				**Acid**			
				BT		**AT**		**BT**		**AT**	
				WN (cm^{-1})	Intensity (AU)	WN (cm^{-1})	Intensity (AU)	WN (cm^{-1})	Intensity (AU)	WN (cm^{-1})	Intensity (AU)
0.5	25	15	12.60	0.3364	1741	6.91E-3	1756 1750 1742 1730	0.01772 0.01953 0.04016 0.03246	1728 1720 1710	4.55E-3 2.29E-3 2.42E-3	1720 1712

BT-Before treatment, AT-After treatment, WN-Wave number

rotation of the C5-C6 covalent bond will again affect the intermolecular hydrogen bond [17,18]. Considering the intramolecular hydrogen bond, a shift in 3335 cm^{-1} (O3H str) to 3339 cm^{-1} and 3456 cm^{-1} (O2H str) to 3454 cm^{-1} respectively is observed. This results in lengthening of O3H···O5 intramolecular hydrogen bond and shortening of the O2H···O6 [17,18]. Another finding from the ATR-FT-IR spectra is that following plasma treatment, the peak at 2853 cm^{-1} (ring C-H stretching) [17] vibrations is shifted to higher frequency 2856 cm^{-1}, indicating that the C-H covalent bond is strengthened and the inter sheet CH···O bond is weakened. The cellulose unit cell experiences strain as a result of these general changes in the hydrogen bond. The overall changes induced in the cellulose are shown in Figure 4.

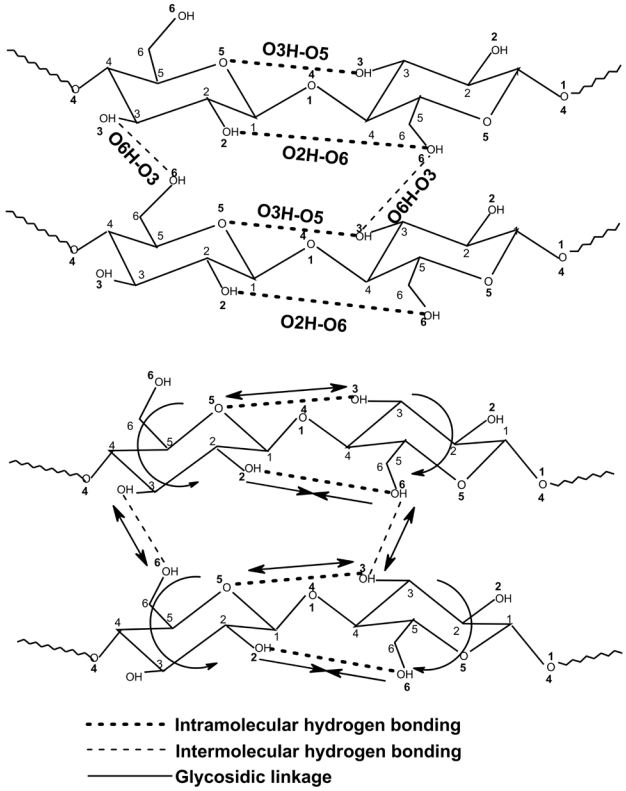

Figure 4. Structural changes due to DC air plasma treatment using optimised process parameters

The weakening of hydrogen bonds has been correlated with the values of LOI, TCI and HBI. It is noted from the Table 2, all the calculated values decrease with plasma treatment which implies that there is a decrease in crystallinity of cellulose. These changes after plasma treatment generate free hydroxyl groups. These accessible hydroxyl groups are easily prone to oxidation when in contact with the plasma species. This has been confirmed from the spectral range between 1740 cm^{-1} to 1710 cm^{-1} where the increase in intensity of C=O peak has been observed after plasma treatment. The four possible sites for oxidation in a cellulose molecule are C_1, C_2, C_3 and C_6 [19,20].

McCord *et al.* (2003); Ward *et al.* (1979) [19,20] have suggested five possible oxidation mechanisms that are as follows: (i) bond breakage between C_1 and glycosidic bond oxygen, (ii) dehydrogenation and dehydroxylation between C_2 and C_3 after the ring opening of anhydroglucose, (iii) bond breakage between C_1 and ring oxygen (iv) dehydrogenation at C_6, (v) dehydroxylation at C_6, bond breakage between C_1 and ring oxygen. The peaks corresponding to 1157 cm^{-1} and 895 cm^{-1} in both spectra are identical in strength, confirming the absence of chain scission or ring opening, as shown in Figure 2 and hence oxidation doesn't occur at C_1, C_2 and C_3 sites. Hence it has been confirmed that oxidation is due to dehydrogenation at C_6. Increase in intensity of C=O peaks implies that more polar groups have been generated and hence there is an increase in hydrophilicity.

3.2 FESEM Analysis of Optimised Sample

A scanning electron microscope is used to examine the surface morphology of control and DC air plasma treated samples. Figure 5 shows FESEM micrographs of untreated and DC air plasma treated cotton fabric at magnifications of 250× and 50000× respectively.

It can be shown that when energetic charged particles in the plasma interact with the fabric, they cause not only chemical and structural changes on the sample surface, but also physical changes such as increase in the existing pore dimension, etching and the formation of micro cavities. By comparing the surface morphology and pore size of the untreated and plasma-treated samples, these alterations can be explained.

The FESEM micrograph of untreated (control) fabric of 250× magnification elucidate that the voids between the warp and weft in the fabric are not open. There are a lot of fibers running across the voids present between the warp and the weft. It is clear from the Figure 5, that the plasma treatment removes the thin hair like fibers running across the warp and weft increasing the void space between warp and weft. The etching of fiber surface after plasma treatment is also evident from Figure 5.

The increase in pore dimension has been quantified by calculating mean pore radius (Table 3) using modified Lucas Washburn Equation (1).

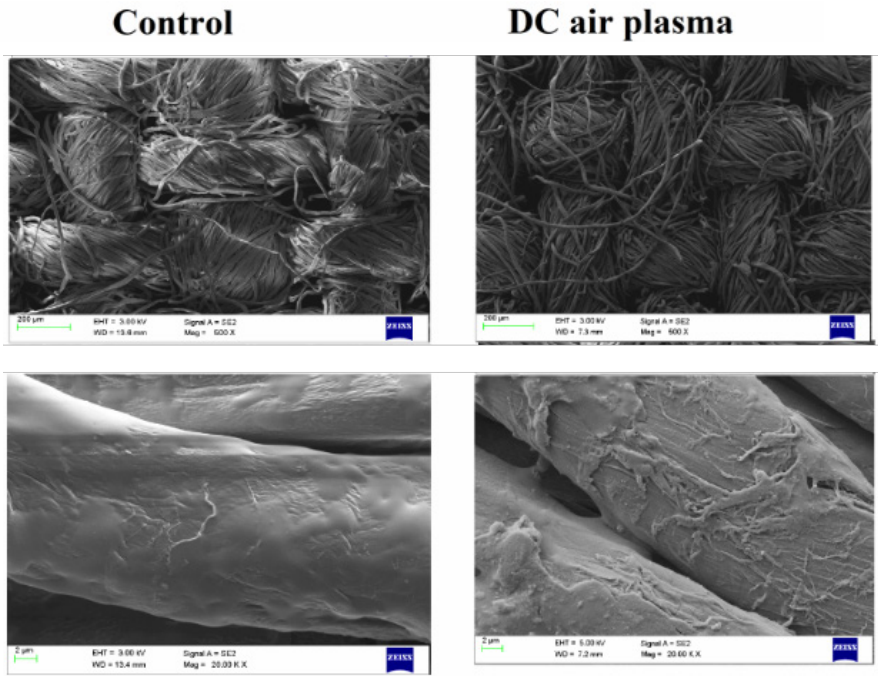

Figure 5. FESEM micrographs of control and DC air plasma (optimised process parameters) treated fabric

Table 3. Mean pore radius of control and DC air plasma (optimised process parameters) treated sample

Sample	Mean pore radius (μm)
Control (untreated)	0.117
DC plasma treated sample	0.336

The results of mean pore radius suggest that bombarding the fabric surface with plasma particles raises the mean pore size, improving the capillarity of cotton fabric and thus enhancing the fabric's hydrophilicity. These findings are consistent with those of Pandiyaraj and Selvarajan (2008) [21].

3.3 Ageing Analysis of DC Air Plasma Treated Cotton Fabric

Investigations are carried out on ageing of plasma treated samples. The wicking height of fabric depends on the concentration of carboxyl content. The wicking ability of the sample increases with increase in carboxyl content and hence plasma treatment promotes oxidation and this leads to an increase in concentration of carboxyl group which was tabulated in Table 4. Even though the plasma treatment improves hydrophilic nature of the fabric, it is necessary to analyze the ageing effect of the fabric. Hence the wicking ability of the samples stored in open air was measured after a week and a month period. In addition, the quantification of carboxyl content and ATR-FTIR analysis was carried out in order to validate the results of variation in wicking height.

The concentration of carboxyl group has increased in DC air plasma treated cotton samples after a seven-day and one-month ageing period, as shown in the Table 4. Upon ageing, the free radicals formed due to plasma treatment react with oxygen in the atmospheric air in turn generates more carbonyl and carboxyl groups leading to oxidation of primary hydroxyl groups on the surface of the fabric [22]. Figure 6 shows an increase in the intensity of peaks at 1740 cm^{-1}~1710 cm^{-1} corresponding to C=O stretching, which confirms the oxidation process.

Table 4. Ageing analysis of DC air plasma treated cotton cellulose

Sample	DC Plasma Treatment			
	WH (cm)	Carboxyl content meq/100 g	Absorbance ratio $\frac{\text{C-C}}{\text{C-O-C}}$	Intensity of Ring CH stretching
Control	9.20	1.561	1.698	1.200E-3
On the day of plasma treatment	12.60	1.613	1.817	5.395E-4
One week after ageing period	11.90	1.701	1.976	1.078E-3
One month after ageing period	10.80	2.137	2.085	6.144E-4

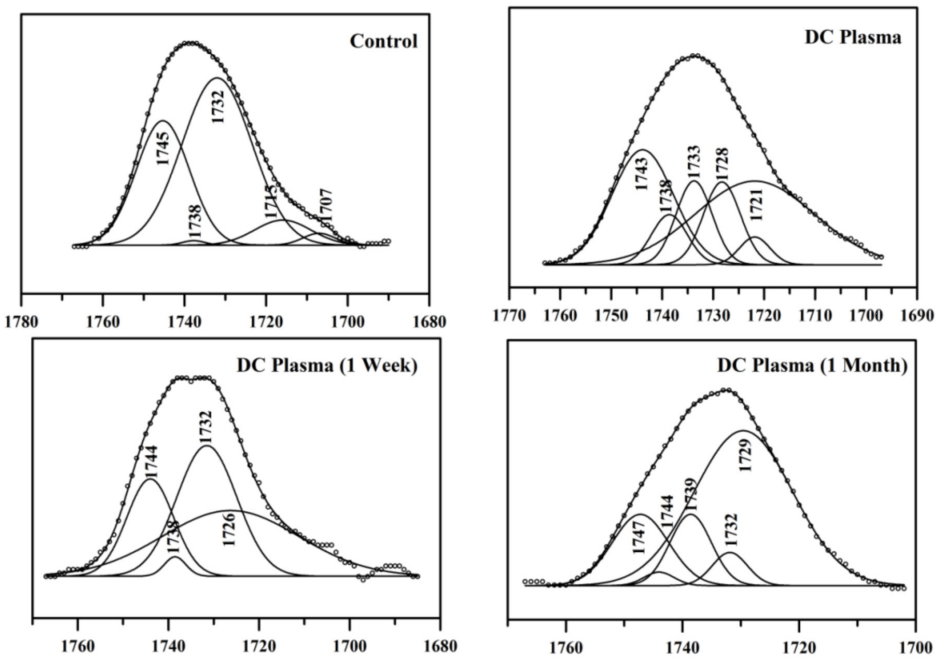

Figure 6. Deconvolution of C=O peaks for DC air plasma treated sample

The increase in carboxyl content concentration due to ageing develops an electronegative potential on the fabric surface which repel the anions through electrostatic repulsion phenomenon thereby decreasing the water uptake capacity [23].

Another possibility might be due to surface reversibility which could be due to either surface reorientation of low molecular weight oxidized materials (LMWOM) into bulk polymer or the reaction of free radicals with new groups or the environment [24]. However, from the IR spectra it can be observed that there was a significant increase in absorbance ratio of $\frac{\text{c-c}}{\text{c-o-c}}$ (Table 4) which is related to the concentration of the C-C component.

The absorbance ratio was determined by dividing the absorbance of C-C band frequency, i.e. 1100 cm^{-1} by absorbance of C-O-C frequency (glycosidic bond, 1158 cm^{-1}) which was used as an internal reference. Parallely, a slight decrease in concentration of ring CH (2850 cm^{-1}) was observed which is evident from the Table 4 and Figure 7.

The increase in absorbance ratio and decrease in concentration of ring CH reveals the fact that with ageing the formation of aliphatic carbon- carbon single bond increases.

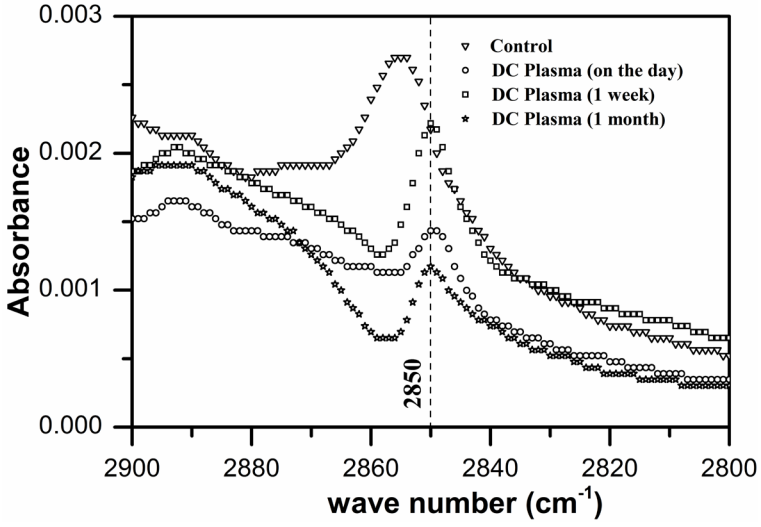

Figure 7. Ageing analysis with reference to the concentration of ring CH

This might be due to the reaction of free radicals with the ambient environment which leads to the transformation of surface polarity. During plasma treatment, reactive species such as H^+ and H^{2+} in the gas mixture bombard the surface of the fabric. As a result, the free radicals are formed on the surface of the fabric by eliminating an atom from a saturated compound as shown in Equation (6) and these free radicals on the polymer chain combines together [25] as shown in Equation (7).

$$-C\text{-}C\text{-}H + H^+ \longrightarrow -C\ -C\ + H_2^+ \quad (6)$$

$$2\text{-}C\text{-}C \longrightarrow -\ C\text{-}C\text{-}C\text{-}C\text{-} \quad (7)$$

The Equation (6) reveals the formation of free radicals on the fabric surface when subjected to plasma treatment and this has been substantiated through IR analysis wherein, decrease in concentration of ring CH is observed which indicates the formation of free radicals in the cellulose chain. These free radicals combine with the radicals which are generated on the neighbouring chain to form carbon-carbon single bond during storage period as depicted in Equation (6). These bonds hinder the diffusion of water through the surface. The formation of aliphatic hydrocarbon has been proved in IR analysis with increase in absorbance ratio of $\frac{C\text{-}C}{C\text{-}O\text{-}C}$. Thus with ageing effect, wettability of the fabric decreases because of the cross links.

Thus the ageing studies reveal that the cellulose structure is affected drastically upon storage, emphasizing that any post treatments should be immediately carried out after the plasma treatment.

4. Conclusions

The cotton fabric was treated with DC air plasma to modify the fabric's surface and the process parameters were optimised using the Box-Behnken design to obtain maximal wicking response. The samples were treated with plasma under optimised conditions suggested by the software and the structural and morphological changes have been analyzed using FESEM and ATR - FTIR studies. The ATR-FTIR study demonstrates the formation of free OH groups due to weakening of intermolecular and intramolecular hydrogen bonds that hold the chain together. This is reflected in the decrease in LOI, HBI and TCI values. Further, the generated free hydroxyl group oxidized to form new carboxylic acid (C=O) peaks which are more polar in nature. DC plasma treatment improves the capillary action by etching process. Due to the DC air plasma treatment, these alterations were caused on the fabric to enhance the hydrophilic nature of the fabric. FESEM analysis confirms the surface roughness and size of micro cavities in the fabric have increased as a result of the DC plasma treatment.

Ageing effect of plasma treated samples was investigated and it was noted that the aged samples were oxidized due to exposure to open atmosphere which was ascertained through carboxyl test and IR analysis. The increased carboxyl content decreases the wickability due to two possible mechanisms (i) electronegative potential developed on the surface repels the anions thereby decreasing the water uptake capacity and (ii) reversibility of surface polarity due to free radical formation which promoted the formation of C-C bonds thereby decreasing the wickability. Thus the ageing studies indicate that the plasma pretreated fabric has to be immediately processed for further studies.

Acknowledgements

The authors wish to thank the Management and Principal, PSG College of Technology, Coimbatore for providing the necessary infrastructure to carry out the study.

Conflict of Interest

There is no conflict of interest.

References

[1] Prabhakaran, M., Carneiro, N., 2005. Effect of low temperature plasma on cotton fabric and its applications to bleaching and dyeing. Indian Journal of Fibre Textile Research. 30, 68-74.

[2] Lee, C.M., Kubicki, J.D., Fan, B., et al., 2015. Hydrogen-bonding network and OH stretch vibration of cellulose: comparison of computational modeling with polarized IR and SFG spectra. The Journal of Physical Chemistry B. 119(49), 15138-15149.

[3] Khai, D.M., Nhan, P.D., Hoanh, T.D., 2017. An investigation of the structural characteristics of modified cellulose from acacia pulp. Vietnam Journal of Science and Technology. 55(4), 452-460.

[4] O'Connor, R.T., DuPré, E.F., Mitcham, D., 1958. Applications of infrared absorption spectroscopy to investigations of cotton and modified cottons: Part I: Physical and crystalline modifications and oxidation. Textile Research Journal. 28(5), 382-392.

[5] Nelson, M.L., O'Connor, R.T., 1964. Relation of certain infrared bands to cellulose crystallinity and crystal lattice type. Part II. A new infrared ratio for estimation of crystallinity in celluloses I and II. Journal of Applied Polymer Science. 8(3), 1325-1341.

[6] Gaur, R., Semwal, S., Raj, T., et al., 2017. Intensification of steam explosion and structural intricacies impacting sugar recovery. Bioresource Technology.

241, 692-700.

[7] Poletto, M., Ornaghi, H.L., Zattera, A.J., 2014. Native cellulose: structure, characterization and thermal properties. Materials. 7(9), 6105-6119.

[8] El-Zawahry, M.M., Ibrahim, N.A., Eid, M.A., 2006. The Impact of Nitrogen Plasma Treatment upon the Physical-Chemical and Dyeing Properties of Wool Fabric. Polymer-Plastics Technology and Engineering. 45(10), 1123-1132.
DOI: https://doi.org/10.1080/03602550600728943

[9] Malek, R.M., Holme, I., 2003. The effect of plasma treatment on some properties of cotton. Iranian Polymer Journal. 12, 271-280.

[10] Kalogianni, E.P., Savopoulos, T., Karapantsios, T.D., et al., 2004. A dynamic wicking technique for determining the effective pore radius of pregelatinized starch sheets. Colloids and Surfaces B: Biointerfaces. 35(3-4), 159-167.

[11] Pandiyaraj, K.N., Selvarajan, V., 2008. Non-thermal plasma treatment for hydrophilicity improvement of grey cotton fabrics. Journal of Materials Processing Technology. 199(1-3), 130-139.

[12] Struszczyk, H., 1986. Modification of lignins. III. Reaction of lignosulfonates with chlorophosphazenes. Journal of Macromolecular Science—Chemistry. 23(8), 973-992.

[13] Pimentel, G.C., Sederholm, C.H., 1956. Correlation of infrared stretching frequencies and hydrogen bond distances in crystals. The Journal of Chemical Physics. 24(4), 639-641.

[14] Nada, A.A.M., Kamel, S., El-Sakhawy, M., 2000. Thermal behaviour and infrared spectroscopy of cellulose carbamates. Polymer Degradation and Stability. 70(3), 347-355.

[15] TAPPI Standards: Regulations and Style Guidelines, 1977. https://www.tappi.org/globalassets/documents/standards/tm_guidelines_complete.pdf. Carboxyl Content of Pulp, T 237 os-77, 1-7.

[16] Anitha, S., Vaideki, K., Prabhu, S., et al., 2019. ATR-FTIR analysis on the hydrogen bonding network and glycosidic bond of DC air plasma processed cellulose. Journal of Molecular Structure. 1180, 378-391.

[17] Altaner, C.M., Horikawa, Y., Sugiyama, J., et al., 2014. Cellulose I_β investigated by IR-spectroscopy at low temperatures. Cellulose. 21(5), 3171-3179.

[18] Nishiyama, Y., Langan, P., Chanzy, H., 2002. Crystal structure and hydrogen-bonding system in cellulose I_β from synchrotron X-ray and neutron fiber diffraction. Journal of the American Chemical Society. 124(31), 9074-9082.

[19] McCord, M.G., Hwang, Y.J., Qiu, Y., et al., 2003. Surface analysis of cotton fabrics fluorinated in radio-frequency plasma. Journal of Applied Polymer Science. 88(8), 2038-2047.

[20] Ward, T.L., Jung, H.Z., Hinojosa, O., et al., 1979. Characterization and use of radio frequency plasma-activated natural polymers. Journal of Applied Polymer Science. 23(7), 1987-2003.

[21] Pandiyaraj, K.N., Selvarajan, V., 2008. Non-thermal plasma treatment for hydrophilicity improvement of grey cotton fabrics. Journal of Materials Processing Technology. 199(1-3), 130-139.

[22] Golova, O.G.P., Nosova, N.I., 1973. Degradation of cellulose by alkaline oxidation. Russian Chemical Reviews. 42(4), 327-333.

[23] Malek, R.M., Holme, I., 2003. The effect of plasma treatment on some properties of cotton. Iranian Polymer Journal. 12, 271-280.

[24] Kolářová, K., Vosmanská, V., Rimpelová, S., et al., 2013. Effect of plasma treatment on cellulose fiber. Cellulose. 20(2), 953-961.

[25] Kan, C.W., Yuen, C.W.M., 2006. Low Temperature Plasma Treatment for Wool Fabric. Textile Research Journal. 76, 309-314.